The hydrological performance of bioretention cells in regions with cold climates: seasonal variation and implications for design

Kim H. Paus, Tone M. Muthanna and Bent C. Braskerud

ABSTRACT

Three bioretention cells in Norway were monitored for 23 to 36 months to evaluate the hydrological performance of bioretention cells operated in regions with cold climates and to test if cell size equations can be used to predict hydrological performance. Values of saturated hydraulic conductivity (K_{sat}) were determined for separate events by analyzing the observed infiltration rates and via infiltration tests. The two cells with the highest K_{sat} values (15.9 and 45.0 cm/h) performed excellently during the study period infiltrating nearly all of the incoming runoff. In contrast, the cell with low K_{sat} value (1.3 cm/h) infiltrated barely half of the incoming runoff. The latter cell had a clear seasonal variation in hydrological performance relating to changes in the K_{sat} values over the year. The size equation that gave the best predictions of the observed hydrological performance accounts for both surface storage and infiltration. By using this equation to evaluate various bioretention cell designs, it was found that the most effective way to increase the hydrologic performance is to have a K_{sat} value above 10 cm/h.

Key words | bioretention, cold climate, infiltration, raingarden, saturated hydraulic conductivity, stormwater management

Kim H. Paus (corresponding author)
Tone M. Muthanna
Department of Hydraulic and Environmental Engineering,
Norwegian University of Science and Technology,
S.P. Andersensv. 5,
7491 Trondheim,
Norway
E-mail: kim.paus@ntnu.no

Bent C. Braskerud
City of Oslo, Water and Sewerage Works,
PO Box 4704 Sofienberg,
N-0506 Oslo,
Norway

INTRODUCTION

Bioretention cells (also referred to as biofilters or rain-gardens) have become a popular urban stormwater management practice in the United States and increasingly are being applied in other parts of the world. Recent research has shown that bioretention cells can reduce stormwater runoff volumes and delay and reduce discharge peaks via infiltration (Hunt et al. 2006; Davis 2008), while simultaneously removing pollutants such as suspended solids, toxic metals, and petroleum hydrocarbons from stormwater (Davis et al. 2003, 2009; Hunt et al. 2008; LeFevre et al. 2012, 2014; Paus et al. 2014a).

In spite of their potential for mitigating stormwater quantity and quality concerns, bioretention cells have not been widely adapted as a stormwater management practice in regions with cold climates. Recent studies have shown, however, that good to excellent removal of pollutants can be achieved also at low temperatures. For example, Muthanna et al. (2007) investigated removal of toxic metals during cold and warm periods in a pilot-sized bioretention box in Trondheim, Norway. The mass reductions of copper, lead, and zinc were reported to be 72% or greater for both periods. Furthermore, in Blecken et al. (2007, 2011), the influence of temperature on nutrient treatment efficiency and total and dissolved metal removals were investigated in vegetated biofilter mesocosms at various temperatures ranging from 2 to 20 °C in the laboratory. Overall, low temperature did not negatively affect the removal of particle-bound pollutants, phosphorus, cadmium, copper, lead, and zinc, resulting in removal rates varying from 46 to 99%. Paus et al. (2014c) investigated the breakthroughs of dissolved cadmium, copper, and zinc at 3.6 and 19.4 °C in columns containing varying amounts of

sand and leaf compost. Only the removal of particulate-phase copper was reported to be negatively influenced by low temperature.

Furthermore, there are reports showing promising results for hydrological performance (Muthanna *et al.* 2008; LeFevre *et al.* 2009; Khan *et al.* 2012). Although these studies strengthen the use of bioretention cells in cold climate regions, there is a lack of hydrological results for in-service and full-scale bioretention cells in cold climates. In particular, little interest has been shown regarding the saturated hydraulic conductivity (K_{sat}) of the engineered bioretention media through which the stormwater infiltrates. The K_{sat} value is a measure of the hydraulic capacity of the cell and is influenced by physical characteristics, including the composition and bulk density of the bioretention media (Thompson *et al.* 2008; Paus *et al.* 2014a), vegetation (Hatt *et al.* 2009; Paus *et al.* 2014b), and the extent of clogging by fine sediments in the incoming runoff (Langergraber *et al.* 2003; Li & Davis 2008). In regions with cold climates, the K_{sat} value may also be significantly negatively influenced by low temperatures (Braga *et al.* 2007; Emerson & Traver 2008), ice and frost in the bioretention media (Khan *et al.* 2012), and the mechanical impacts on soil structure from freeze–thaw cycles (Asare *et al.* 1999). Finally, road salts (e.g., NaCl) may not only reduce removal and facilitate mobilization of toxic metals in bioretention cells (Paus *et al.* 2014c; Søberg *et al.* 2014; Szota *et al.* 2015), but can also change the soil structure, resulting in significant reduction of the K_{sat} value (Kakuturu & Clark 2015). When targeting the hydraulic capacity of bioretention cells in cold climates, these variations on the K_{sat} value must be considered.

The overall aim of this study was to evaluate the effects of season and temperature on the K_{sat} value and hydrological performance of bioretention cells operated in cold climates. Furthermore, it was hypothesized that cells in cold climate regions require a K_{sat} value above a certain threshold level to function satisfactorily. Results from three full-scale bioretention cells continuously monitored over the course of 2 to 3 years in Trondheim and Oslo, Norway, are reported. The recorded hydrological data were used to test various size equations and finally to evaluate how design parameters can optimize bioretention cell performance.

METHODOLOGY

Site descriptions

The three pilot bioretention cells assessed in this study are located in residential areas at Risvollan, Trondheim (RIS), Langmyrgrenda 34B, Oslo (L34B), and Nils Bays vei 21, Oslo (NB21). Photographs and illustrations of the cells are given in the Appendix, Figure S1 (available with the online version of this paper) and in Braskerud *et al.* (2013). The cells were constructed for research purposes and were sized to manage water from catchments with impermeable areas 10 to 20 times larger than the cell surfaces. All cells were planted with a great variety of species, mainly perennials and ferns. In total, more than 30 species were planted in the cells (e.g., *Carex* spp., *Alchemilla mollis*, *Filipendula* spp., *Iris* spp., *Rodgersia aesculifolia*, *Lythrum salicaria*). Water flows in and out of the cells and surface water levels were monitored using sharp V-notch weirs with pressure sensors. The design, instrumentation details, and the physical and chemical characteristics of the bioretention media are, for the three cells, summarized in Table 1 and briefly described in the following.

The RIS site was constructed to retain and detain the runoff from a large catchment before it is discharged to the municipal stormwater system. The catchment consists of asphalt and grass with underlying clay, thus effective infiltration in the catchment is largely restricted. The cell was constructed with bioretention media made by mixing commercial construction sand, leaf compost, and local topsoil. The media bed depth and maximum ponding height were set to 75 cm and 16 cm, respectively. Two perforated 100 mm diameter PVC drain pipes with 5% slope convey infiltrated water to the outlet. In order to obtain control of the water balance, the cell was lined with a 1.5 mm thick polypropylene membrane.

The L34B site was constructed to manage water locally from a driveway. The bioretention media were composed of local topsoil with high infiltration rate, hence no amendments were used at L34B. A brim built around the cell allowed a maximum water height of 6.5 cm to be stored. L34B is not drained by pipes and infiltrated water percolates to well-drained surrounding soils of sandy loam moraine.

Table 1 | Design and media characteristics of the three bioretention cells assessed in this study. Additional photographs and design configurations are available in the Appendix (Figure S1, available with the online version of this paper) and in Braskerud et al. (2013)

	RIS	L34B	NB21
Design characteristics			
Location	Risvollan, Trondheim	Nordberg, Oslo	Sogn, Oslo
Year constructed	2010	2006	2009
Drainage area type	13% asphalt and 87% grass	46% asphalt, 30% gravel road, and 24% grass	100% roof
Drainage area (A)	8,300 m^2	291 m^2	139 m^2
Surface area (A_{bio})	40.0 m^2	5.9 m^2	10.3 m^2
Surface to drainage area (A_{bio}/A)	0.5%	2.0%	7.4%
Surface to impermeable area	4.3%[a]	16.0%[a]	8.2%[b]
Maximum ponding height (h_{max})	16.0 cm	6.5 cm	20.0 cm
Media bed depth (d)	75.0 cm	–	80.0 cm
Drain pipes	2×100 mm	Not drained	Partly blocked 100 mm
Estimated vegetative cover	60%	>90%	80%
Instrumentation			
Inflow	150° v-notch	90° v-notch	Not monitored
Outflow	120° v-notch	160° v-notch	150° v-notch
Drain	90° v-notch	Not drained	Not monitored
Soil water content	5 cm below surface	5 cm below surface	Not monitored
Soil temperature	5 and 50 cm below surface	5 cm below surface	60 cm below surface
Precipitation	Nearby tipping bucket	Tipping bucket at site	Nearby tipping bucket
Media characteristics			
Media composition	70% sand, 25% leaf compost, and 5% topsoil	100% topsoil	50% sand, 45% leaf compost, and 5% topsoil
Media texture (USDA triangle)	Loamy sand	Sandy loam	Loamy sand
Sand:loam:clay	75:21:3	74:20:6	77:17:6
Effective size (d_{10})	17 μm	6 μm	6 μm
Uniformity coefficient (UC)	19	61	61
Porosity [m^3/m^3]	34%	44%	39%
Bulk density (ρ_b)	1.28 g/cm^3	1.07 g/cm^3	1.18 g/cm^3
Organic matter content (top 15 cm)	4.3%	8.4%	7.8%

[a]Calculated as the product of the bioretention surface area (A_{bio}) and the precipitation depth divided by the cell inflow volume.
[b]Calculated using a roof runoff coefficient of 0.90.

The NB21 site was constructed to retain and detain roof runoff from a private house before it is discharged to the municipal storm sewer system. Runoff is conveyed to the cell inlet through gutters. The bioretention media were composed of commercial construction sand, leaf compost, and local topsoil to a depth of 75 cm. The drainage layer of NB21 is sloped so that the layer is visible at the surface (Appendix, Figure S1). The purpose of this design was to facilitate infiltration through the cell during periods when solid frost is developing in the organic matter-rich bioretention media. The maximum ponding height on the surface was set to 20 cm. The surrounding soil is dominated by

clay and a drain pipe, perforated below the media depth of 70 cm, which drains the cell. The bottom end of the pipe was partly blocked to allow a maximum of 36 L/min to be conveyed to the storm sewer system. Different from the other cells, only water flows out of the cell and surface water levels were monitored at the NB21 site.

Data collection

The pressure sensors used to monitor the water levels in the three cells were AquiStar®PT-12, 4tech UC2, and LevelTROLL®100, for RIS, L34B, and NB21, respectively. The pressure sensor used in NB21 was not designed to record data at temperatures below freezing, hence no winter data were obtained for this site. For all cells, Vegetronix VH400 Soil Moisture Sensor Probes and PT-100 4 wire soil temperature sensors were used to monitor the water content and temperature of the bioretention media. Precipitation data were collected using Lambrecht 1518 H3 tipping buckets. Sutron Xlite 9210 data loggers were used to record data at intervals of 1 minute (i.e., pressure transducers and precipitation) and 15 minutes (i.e., soil water content, soil temperatures, and air temperature). The soil moisture sensor probes placed at RIS and L34B were calibrated to develop relationships between the dielectric constant and the volumetric water contents (see Appendix for details, available with the online version of this paper).

Analytical methods

An Arts Machine Shop soil corer equipped with plastic liners (inner diameter 3.8 cm) was used to collect cores from a depth of 0 to 15 cm at evenly spaced locations throughout the cells. Core collection was carried out at one occasion only for each cell, and was therefore not expected to affect the overall hydraulic capacity of the cell. Cores were brought to the laboratory, dried for 24 hours at 105 °C and sieved using a 2 mm nylon mesh. Particle size distributions were determined using the Pipette method (Krogstad 1992). The organic matter content (OM) in the bioretention media samples was estimated using the loss on ignition (LOI) method (Krogstad 1992). Ten grams of dry media were weighed, combusted at 550 °C for 4 hours, and then weighed again.

Data analysis

Definition of events and hydrologic parameters

The start of a hydrological event was defined as the time water began to flow into the cell. The end of an event was defined as the time when water ceased to flow through the inlet and the pressure sensors located in the bioretention media indicated that water level in the cell was at 30 cm below the surface. All events were divided into three types: (1) rain-on-snow events, when significant rainfall occurred while snow was present in the drainage area; (2) snowmelt events, when no significant rainfall occurred while snow was present in the drainage area; and (3) rain events, when rainfall occurred and no snow was present in the drainage area. Furthermore, the mean hydraulic loading rate was calculated as:

$$HLR = \frac{V_{in}}{A_{bio} \cdot t} \tag{1}$$

where HLR is the mean hydraulic loading rate [m/h], V_{in} is the inflow volume [m³], A_{bio} is the bioretention surface area [m²], and t is the inflow duration for the event [h]. The volume of runoff that infiltrated through the cell (V_{inf}) [m³], was calculated as:

$$V_{inf} = V_{in} - V_{of} \tag{2}$$

where V_{of} is the volume that overflows [m³]. Finally, the fraction of runoff volume infiltrated [%] was calculated as:

$$f_{inf} = \frac{V_{in} - V_{of}}{V_{in}} \tag{3}$$

Saturated hydraulic conductivity

The observed infiltration rates (i.e., the recorded decline in ponded water height over time) were used as estimates of the K_{sat} values. A similar approach of estimating K_{sat} values was used by Emerson & Traver (2008) when monitoring two stormwater infiltration practices at Villnova University, Pennsylvania, USA. The K_{sat} values were estimated for all hydrologic events that satisfied the following

criteria: (1) water ponded on the cell surface; (2) there was no inflow to the cell; (3) the soil moisture sensor probes indicated a completely saturated media; and (4) the recorded data indicated a minimum hydraulic gradient (i.e., ~1 m/m). Clearly, when using the change in ponded water height over time for the estimation of the K_{sat} value, there will always be a hydraulic gradient greater than 1, hence the estimate will consistently be higher than the actual K_{sat} value. Emerson (2008) used the ponding water heights between 24 and 18 cm to estimate the K_{sat} values, and showed via Monte Carlo sensitivity analysis that the K_{sat} values obtained by the Green-Ampt infiltration model were, on average, 81% lower than the K_{sat} values estimated from the observed infiltration rate. Hence, to minimize the influence of the hydraulic gradient on the estimate, only the water heights between 8 and 0 cm were analyzed. At this interval, the ponded water depth versus time data had good linear correlations ($R^2 > 0.90$) for all events analyzed. Although the estimates using this approach may also be influenced by certain factors (e.g., the volume occupied by vegetation on the surface and evapotranspiration) they were deemed sufficient given the scope of this study.

Modified Philip-Dunne (MPD) infiltrometer tests were conducted as a second approach of estimating K_{sat} values of the bioretention media. The MPD test is designed to measure infiltration on the surface of stormwater practices and has previously been used for estimating K_{sat} values of the bioretention cells (Asleson *et al.* 2009; Paus *et al.* 2014b). The MPD infiltrometer is a falling head device and its design, accuracy/precision, and use are described in detail elsewhere (Nestingen 2007). MPD tests using plastic cylinders with a height of 45 cm and an inner diameter of 10 cm were conducted at the three cells during various seasons (i.e., nine, three, and two occasions at RIS, L34B, and NB21, respectively). The number of simultaneous tests conducted at each sample occasion ranged from 3 to 17, resulting in a mean spatial resolution of 2 m^2 cell surface per test. To evaluate the effect of temperature on infiltration, K_{sat} estimates versus temperature were plotted and compared with the following theoretical relationship (Hillel 1998):

$$K_{sat} = k\frac{\rho \cdot g}{\mu} \tag{4}$$

where k is the intrinsic media permeability [cm^2], ρ is the density of the fluid [g/cm^3], g is the gravitational acceleration [cm/h^2], and μ is the dynamic viscosity [g/(cm h)]. Table values from Crowe *et al.* (2005) were used to calculate μ and ρ at the temperature recorded.

Evaluation of size equations

Rearranged versions of the four simple bioretention size equations that were used to predict the hydrological performance at the two cells where inflow runoff was monitored (RIS and L34B) are listed in Table 2. For each rain event, Equations (5)–(8) were used to calculate the volume infiltrated (V_{inf}) given the recorded inflow volume (V_{in}) and duration (t) of inflow, the estimated K_{sat} values, and the cell specifics given in Table 1. The equations were evaluated by performing linear regression analyses on the observed versus predicted V_{inf} values using Minitab® 16.1.0 (Minitab 2010).

RESULTS AND DISCUSSION

Hydrological performance and K_{sat} values of the three cells

In total, 119 and 173 hydrological events were identified for RIS and L34B during the study period (Table 3). The capacity of RIS to capture and infiltrate the incoming runoff was considerably lower than the capacities of L34B and NB21. For example, overflow occurred for 26% of the events at RIS, while at L34B, overflow was recorded only for 1% of the events (i.e., short-term heavy precipitation during summer), and never at NB21.

The variation in hydrological performance among cells was attributed to bioretention cell characteristics. To illustrate the difference between RIS and L34B, the hydrologic responses to two rain events of the same magnitude (i.e., 31 and 28 mm) are shown in Figure 1. The antecedent number of dry days before these events was 5 and 7 days for RIS and L34B, respectively, hence the initial soil conditions were relatively equal. The first inflow peaks resulted in a rise in media water contents which leveled out at their saturated values at both cells. At RIS, water began to pond

Table 2 | Size equations used to predict the runoff volume infiltrated (V_{inf}) at RIS and L34B

Equation		Description and assumptions
$V_{inf} \leq A_{bio} \cdot h_{max}$	(5)	An equation proposed by Hunt & White (2001) where the capacity to infiltrate runoff equals the above surface volume ($A_{bio} \cdot h_{max}$) and where infiltration is not accounted for
$V_{inf} \leq A_{bio}(h_{max} + n \cdot d)$	(6)	An equation used to size cells in *New York State Stormwater Management Design Manual* (NYSDEC 2010). The capacity to infiltrate runoff equals the sum of the above surface volume ($A_{bio} \cdot h_{max}$) and the below surface pore volume ($A_{bio} \cdot n \cdot d$). The equation assumes that the infiltration rate through the surface is not limiting the water movement
$V_{inf} \leq A_{bio} \cdot t \cdot K_{sat} \cdot \dfrac{(h+d)}{d}$	(7)	A derivation of Darcy's law commonly used to design sand filters (Austin 1988) and bioretention cells (Claytor & Schueler 1996; PGC 2007). Because the hydraulic gradient ($(h+d)/d$) is already incorporated in the K_{sat} estimate in this study, the hydraulic gradient is assumed to be 1. The capacity to infiltrate runoff equals the volume that is able to infiltrate ($A_{bio} \cdot K_{sat} \cdot t$) over the duration of inflow
$V_{inf} \leq A_{bio} \cdot (h_{max} + K_{sat} \cdot t)$	(8)	An equation proposed by Paus & Braskerud (2014) where the capacity to infiltrate runoff equals the sum of the above surface volume ($A_{bio} \cdot h_{max}$) and the volume that is able to infiltrate ($A_{bio} \cdot K_{sat}$) over the duration of inflow (t)

V_{inf} is the runoff volume infiltrate [m³], A_{bio} is the bioretention surface area [m²], h_{max} is the maximum height of ponded water on the surface [m], h is the average height of ponded water on the surface [m], n is the mean effective porosity in the bioretention media, d is the bioretention media depth [m], K_{sat} is the saturated hydraulic conductivity [m/h], and t is the inflow duration [h].

Table 3 | Summary of hydrological events for RIS, L34B, and NB21. Hydraulic loading rates (HLR) and saturated hydraulic conductivities (K_{sat}) are given as the mean ± the standard deviation

	RIS	L34B	NB21
Duration of study period	36 months (6 June 2011 to 5 June 2014)	36 months (18 June 2010 to 26 June 2013)	23 months (11 July 2011 to 24 June 2013)
Total inflow [cm]	3,053	1,147	
Total overflow [cm]	1,351	20	0
Fraction of volume infiltrated, f_{tr} [%]	55%	98%	100%
No. of rain events	102	161	–
No. of snowmelt events	11	7	–
No. of rain-on-snow events	6	5	–
No. of events with ponded water	65	6	7
No. of events with overflow	31	2	0
Mean HLR [cm/h]	1.8 ± 1.5	1.5 ± 2.7	–
Mean K_{sat} (OIR) [cm/h][a]	1.3 ± 0.7	45.0 ± 15.3	15.9 ± 16.9
Geo mean K_{sat} (MPD) [cm/h][b]	2.4	49.8	23.5
Mean K_{sat} (MPD) [cm/h][b]	5.0 ± 5.7	52.5 ± 23.7	31.5 ± 26.7

[a]Estimated from the observed infiltration rates (OIR) during rain events.
[b]Estimated from the MPD infiltrometer tests.

almost immediately on the surface. The second inflow peak resulted in a further rise of ponded water, and finally, the water height exceeded the maximum level of 16.0 cm and the cell overflowed. After the inflow ceased, the ponded water infiltrated at a relatively constant rate (i.e., 1.7 cm/h) over 9 hours and the water content began to decline after

another 4 hours. The outflow rate at RIS remained relatively constant until all surface water had infiltrated. For L34B, ponding did not occur during the first inflow peak. At the end of the second inflow peak, the surface water height rapidly rose above the maximum level of 6.5 cm resulting in overflow. After the inflow ceased, all surface water infiltrated within approximately 6 minutes (i.e., rate of 60.1 cm/h). In these particular events, the mean HLR was considerably higher for L34B (i.e., 20.4 cm/h) than for RIS (i.e., 2.9 cm/h), yet, due to the high infiltration rate, L34B managed a much higher fraction of the inflow.

The observations in Figure 1 clearly illustrate that the hydrological performance of a bioretention cell is significantly affected by the infiltration rate. The mean K_{sat} values estimated from the observed infiltration rate (OIR) indicate the following order of hydraulic capacity: L34B > NB21 > >RIS (Table 3). In general, the range in K_{sat} values reflects previously reported values for bioretention cells (Hunt *et al.* 2006; Asleson *et al.* 2009; Le Coustumer *et al.* 2009; Paus *et al.* 2014b). The results from the MPD infiltration tests support the variation in hydraulic capacities (Table 3). For RIS and NB21, however, the K_{sat} values estimated using the MPD infiltration tests were two to four times higher

than those estimated from the OIR. This could be due to the fact that MPD tests only measure K_{sat} values in the upper 15 to 20 cm, and thus the estimates will not be affected by physical constraints limiting infiltration below this depth (e. g., surrounding soils with lower permeability, too small or clogged drain pipes, and low exfiltration). Obvious constraints at RIS and NB21 are the impermeable barriers surrounding these cells (i.e., liner and clay). While the physical constraints at RIS and NB21 account for some of the variation in K_{sat} values for the three cells assessed, the MPD tests indicate that also the surface infiltration at RIS is considerably lower than for the other two cells. One important factor that can impact the K_{sat} value of bioretention media is clogging by incoming sediments (Langergraber *et al.* 2003; Li & Davis 2008). However, at RIS the drainage area consists of 87% grass, thus suggesting that the incoming sediment load is expected to be minimal. A more likely explanation for the lower K_{sat} value at RIS could be the differences in cells' media characteristics (Table 1). Although the grain size distribution profiles for the media in the three cells are relatively similar (see Appendix, Figure S2, available with the online version of this paper), the higher bulk density at RIS indicates that the media has a higher degree of compaction than the
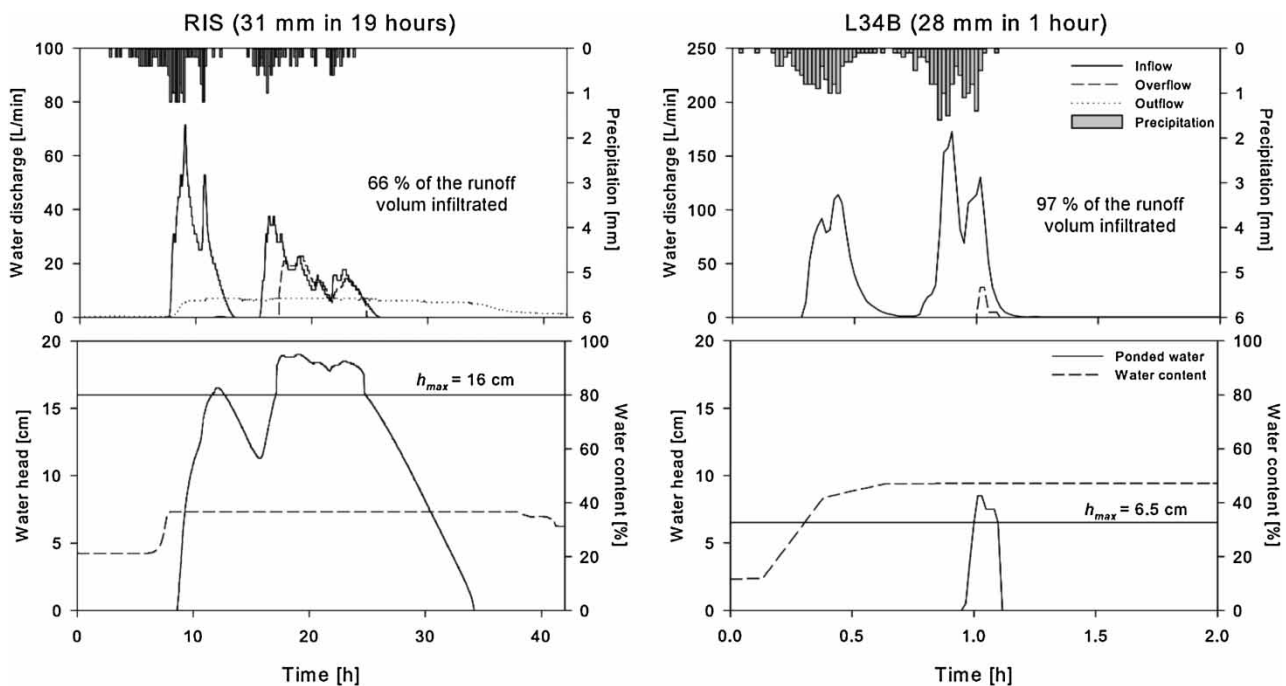

Figure 1 | Precipitation and inflow and outflow hydrographs for RIS (15 August 2011) and L34B (7 June 2011) (upper panel). Surface water head, overflow level (h_{max}), and media water content (lower panel).

media in the two small cells (Table 1). The K_{sat} value is expected to decrease with increasing compaction as water movement becomes more restricted (Gregory *et al.* 2006). During the construction of RIS, an effort was made to ensure a smooth and even cell surface. Although this was carried out with care, it cannot be ruled out that the action resulted in a sufficient degree of compaction to affect the K_{sat} value. Furthermore, also the organic matter (OM) contents are higher and vegetation more established at the two small cells than at RIS (Table 1). Increasing OM content has been reported to positively correlate to increasing K_{sat} values in soils due to its effects on soil aggregation (Hudson 1994; Saxton & Rawls 2006), and activities of insects and earthworms that can enhance water movement through the soil matrix by their development of macropores (Lamande *et al.* 2003). Additionally, vegetation can increase hydraulic capacities as root dieback creates macropores in the soil (Archer *et al.* 2002), and well-established vegetation in bioretention cells has been linked to high K_{sat} values in previous studies (Hatt *et al.* 2009; Paus *et al.* 2014b). The difference in bulk densities, OM contents, and vegetation cover are therefore factors that support the lower K_{sat} values of RIS than at the two small cells.

Influence of season and temperature on the K_{sat} values

Figure 2 shows the monthly mean K_{sat} values for the three cells together with the fraction of infiltrated water for RIS

and L34B. At RIS, there is a clear seasonal variation, with K_{sat} values during winter/early spring (i.e., March to April) and autumn/early winter (i.e., September to December) being only 25 to 43% of those during summer (i.e., June and July). Despite the low number of K_{sat} estimates (missing values represent months without ponding events), similar variation is also apparent for the small cells. The seasonal variation in K_{sat} values is expected as low temperature and/or frost in the bioretention media reduce infiltration during the colder months. By analyzing the 15 K_{sat} values estimated during snowmelt and rain-on-snow events occurring at RIS in March and April, it was found that these estimates had a relatively large variation despite the temperature being very close to freezing point (ranging from 0.0 to 1.1 cm/h). Although not evaluated in this study, the large variation in estimates may be attributed to the extent and type of frost (e.g., porous or concrete frost) developing at the surface and in the bioretention media of the cell.

To investigate the influence of temperature on the K_{sat} values, temperatures in bioretention media (RIS) and air (L34B and NB21) were plotted versus K_{sat} values, in Figure 3. To exclude the influence of frost in the bioretention media, only rain events are analyzed. For all cells, positive linear relationships between the K_{sat} value and temperature were found when performing a linear regression analysis on the data (significant at levels of 0.05). The slopes of the regression lines were consistently greater than the theoretical relationship predicted. At RIS the regression slope (i.e.,
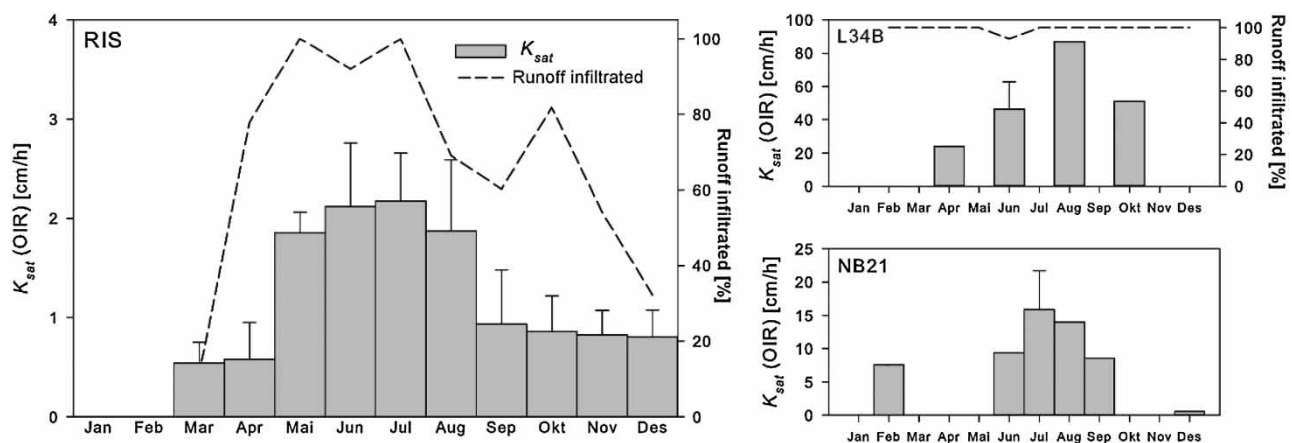

Figure 2 | Monthly mean fraction of runoff volume infiltrated and K_{sat} values estimated from OIR for RIS (left), L34B (top right), and NB21 (bottom right). Fraction of runoff volume infiltrated was not estimated for NB21 as the inflow was not recorded. Missing values represent months without events where water ponded/inflow were recorded.

0.11 cm/h/°C) was more than twice as high as the slope of theoretical relationship (i.e., 0.04 cm/h/°C). Interestingly, the data for RIS show that an overweight of the K_{sat} estimates for the period May to August were above the theoretical relationship, and conversely, that an overweight of the K_{sat} estimates for the period September to November were below the theoretical relationship. This supports that there are physical changes occurring in the media after the winter. For example, it can have been caused by the cracks in the surface crust caused by freeze–thaw cycles (Asare *et al.* 1999) which were typically observed a short time after the ice and snow covering the surface had gone during spring. The variation in K_{sat} estimates caused by physical changes in the media also supports the low R^2 values obtained when K_{sat} values are plotted versus temperature (Figure 3).

Predicting hydrological performance

Equations (5)–(8) in Table 2 were used together with the recorded hydrological data to predict the runoff volume infiltrated at RIS and L34B for each rain event. To investigate if including a temperature-dependent K_{sat} value would improve results, Equations (7) and (8) were additionally applied using the relationships between temperature and K_{sat} from Figure 3. Plots of predicted versus observed runoff volume infiltrated using Equations (5)–(8) are shown for RIS in Figure 4, and results from both cells summarized in Table 4. A regression line slope less than 1 indicates that the equation, on average, predicts a higher V_{inf} value than observed. Practically, this means that the cell, if designed via this equation, will be undersized, and hence there is a greater overflow of water than was intended. Conversely, if the slope is greater than 1, the equation on average predicts a higher V_{inf} value than observed, indicating that a cell designed using this equation will be oversized.

Clearly, by not accounting for infiltration, Equation (5) fails to predict the runoff volume infiltrated for all events with an inflow volume greater than the surface volume (Figure 4). Hence, the use of Equation (5) will result in oversized bioretention cells. Similarly, Equation (6), which has a constant volume capacity (i.e., the surface storage and the below surface pore volume), fails to predict the runoff
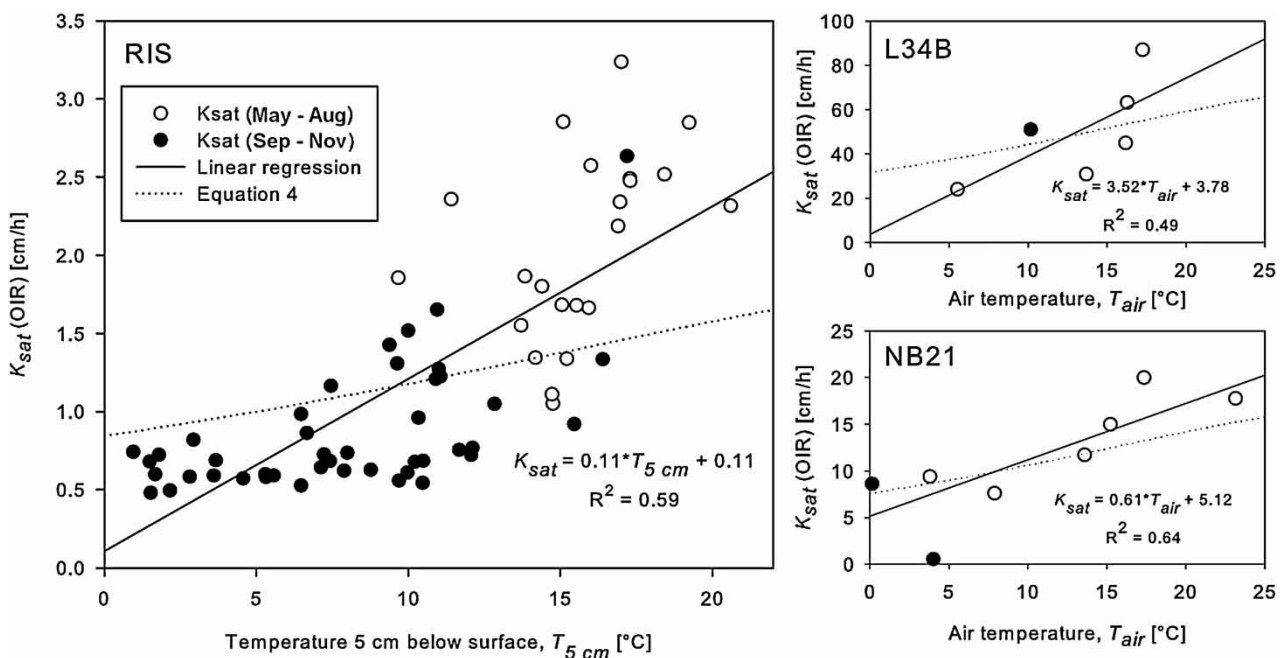

Figure 3 │ Saturated hydraulic conductivity (K_{sat}) estimated by the OIR for rain events versus the temperature 5 cm below the surface (RIS), and air temperature (L34B and NB21). The theoretical relationships were calculated using Equation (4), table values for ρ and μ (Crowe *et al.* 2005), and intrinsic media permeability values of 4.3×10^{-9} cm^2, 161.6×10^{-9} cm^2, and 38.7×10^{-9} cm^2 for RIS, L34B, and NB21, respectively.
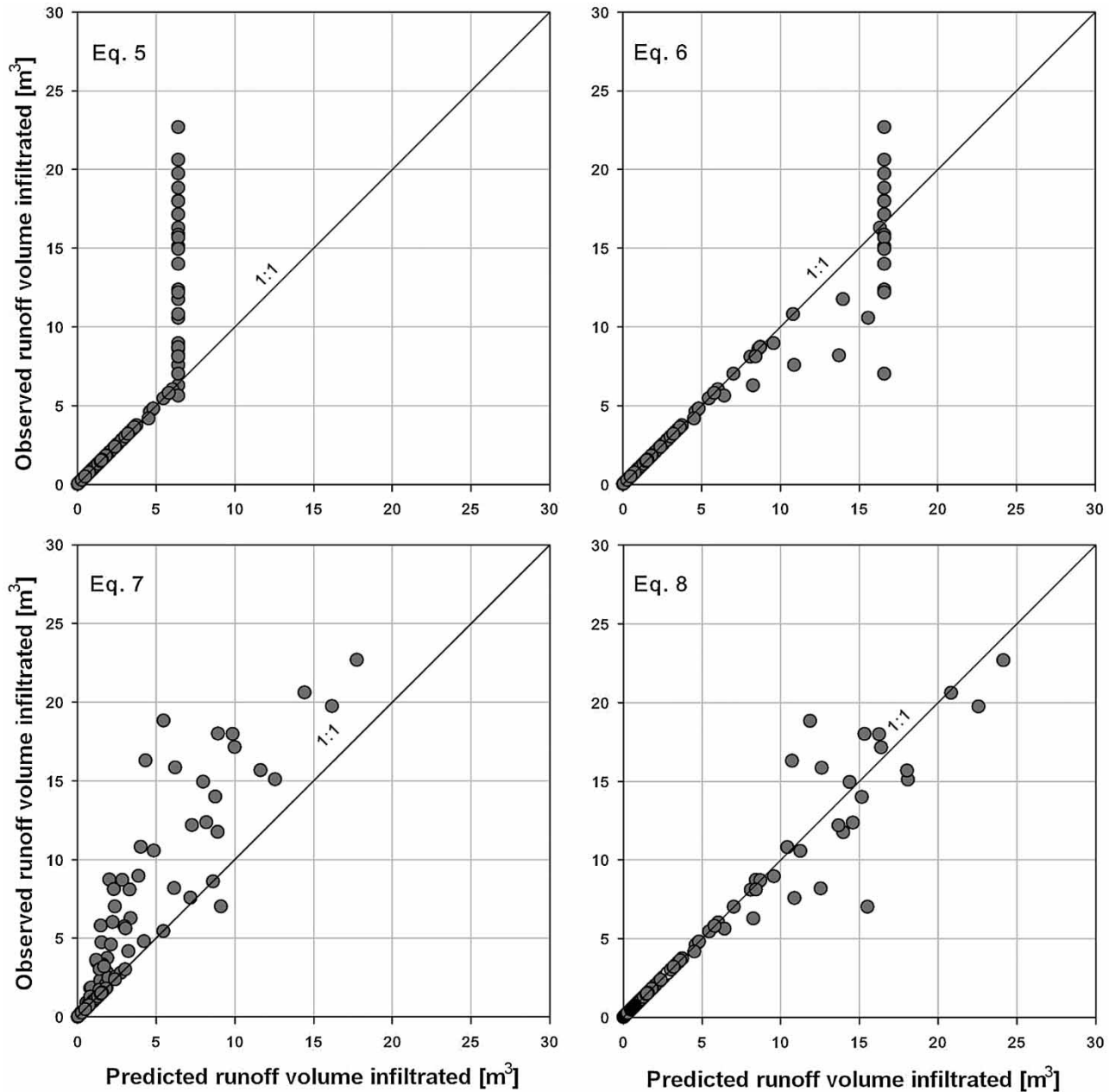
Figure 4 | Predicted runoff volume infiltrated using Equations (5)–(8) versus observed runoff volume infiltrated at RIS.

volume infiltrated for all events with a sufficient inflow volume. Additionally, for inflow volumes between 6 and 15 m³, the predicted values for Equation (6) are consistently equal to or greater than the observed values (Figure 4). Hence, the assumption that the infiltration rate is not restricting the movement of water through the surface may be incorrect. For bioretention cells where the bioretention

media have a low K_{sat} value (e.g., RIS), Equation (6) will result in undersized cells. Furthermore, Equation (7) does not include the above surface storage capacity and therefore fails to predict the runoff infiltrated for events with small- to medium-sized inflow volumes where the hydraulic loading rate typically exceeds the K_{sat} value. Equation (8), which includes both surface storage and infiltration, has the best

Table 4 │ Results from regression analysis between the predicted runoff volume infiltrated using the four size equations and the observed runoff volume infiltrated for sites RIS and L34B

Equation	Infiltration	RIS			L34B		
		Slope	Intercept	R^2	Slope	Intercept	R^2
(5)	None	1.95	−1.15	0.72	2.58	−0.16	0.31
(6)	None	0.94	0.07	0.92	1.23	−0.06	0.85
(7)	Constant	1.41	0.68	0.82	0.97	0.01	0.98
(7)	Temperature[a]	1.29	1.61	0.65	0.97	0.01	0.98
(8)	Constant	0.94	0.14	0.93	0.97	0.01	0.98
(8)	Temperature[a]	0.96	0.30	0.86	0.97	0.01	0.98

[a]K_{sat} values calculated for the mean event temperature using the linear regression equations from Figure 3.

fit to the observed data. Finally, including a temperature-dependent K_{sat} value only marginally improves Equation (8) with respect to the slope, but not the intercept and the R^2 coefficient. Hence, it appears that using an annual average K_{sat} value is sufficient when accounting for the variations in temperature.

Implications for design

The hydrological performance of the bioretention cells assessed in this study would have been different if the cells were designed differently. An increase in the surface area (A_{bio}), the K_{sat} value of the bioretention media, or the maximum level of water on the surface (h_{max}) would all result in a higher hydraulic capacity, and thus a higher fraction of

runoff infiltrated. To investigate the impacts of these three parameters on the hydrological performance, Equation (8) was used to calculate the runoff infiltrated at RIS and L34B for all events with varying one of the three parameters (A_{bio}, K_{sat}, and h_{max}) separately. For each parameter, the fraction of runoff infiltrated was calculated as the accumulated runoff infiltrated divided by the accumulated inflow volume. The results are shown in Figure 5 and illustrate that the most effective way to increase the fraction of water infiltrated at RIS would be to have a K_{sat} value of at least 10 cm/h. With a K_{sat} value of 10 cm/h at RIS, all the inflowing water generated from rain events would infiltrate during the study period. In comparison, by doubling the A_{bio} only 80% of the water would infiltrate. Also, by doubling the h_{max} (i.e., 30 cm) only about 10% more of the
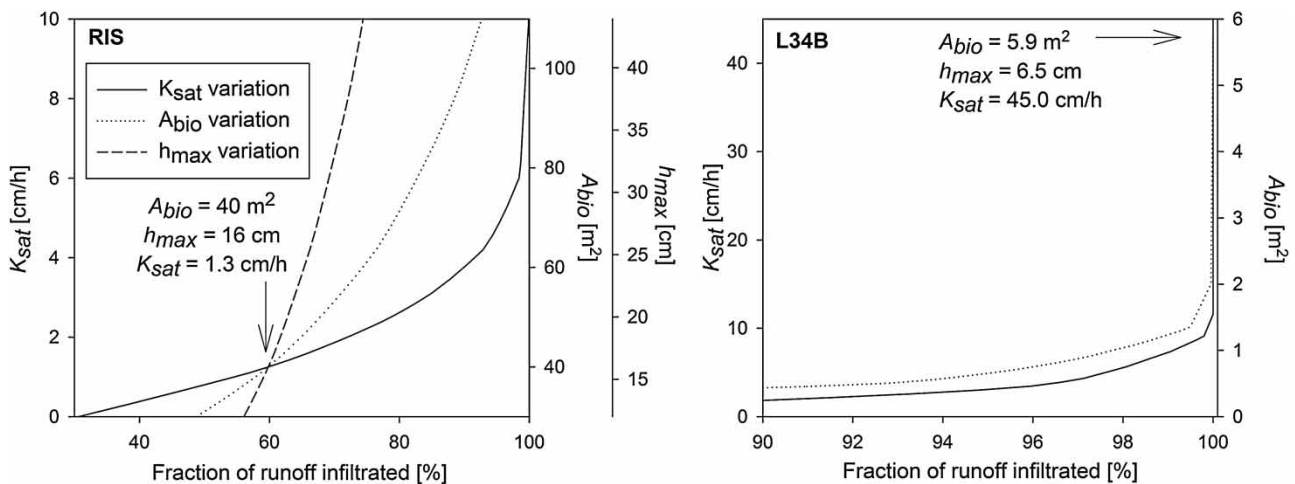

Figure 5 │ Fraction of water volume infiltrated when varying design specifications (h_{max}, K_{sat}, A_{bio}) at RIS and L34B. For RIS, the three curves intercept at the current design at which about 58% of the inflow is infiltrated. The effect of varying the h_{max} value is not shown for L34B because the hydraulic loading rate never exceeded the estimated K_{sat} value.

inflow would infiltrate compared to the current design. For L34B, the cell already has a high hydrological performance. The results indicate, however, the cell is oversized and equally good performance would have been achieved if the cell had a considerably smaller surface area.

From Equation (8) it appears that a high h_{max} value is beneficial when the cell is to be designed for heavy showers with short duration, while a high K_{sat} value (i.e., >10 cm/h) is important when precipitation patterns are recognized by long showers with medium to low intensities. However, it may be practically difficult to target a specific K_{sat} value when designing cells. For bioretention cells operated in cold climates, it is recommended to use a rather coarse bioretention media composition with a high fraction of sand and low fractions of clay and silt to form well-drained cells (Caraco & Claytor 1997; Blecken *et al.* 2011). Additionally, from the experiences gained when constructing and monitoring the cells in this study, it appears important to: (1) use topsoil of good quality (i.e., low clay content); (2) avoid any form of media compaction; (3) ensure that the size of drain pipes does not constrain water movement; (4) consider pre-treatment to avoid particle clogging as a result of sand usage in cold climate regions; and (5) get vegetation well established.

Clearly, the relationships of Figure 5 may be relevant only for the cases in Trondheim and Oslo and thus it is necessary to climatically adapt the design to representative temperature regimes and precipitation patterns. For example, while using an annual average K_{sat} value can be sufficient for cell sizing in Oslo and Trondheim, it may be necessary to include a temperature-dependent K_{sat} value in continental climates where the annual variation in temperatures typically are greater than in coastal climates. Inevitably, also-site specific properties such as the catchment size and slope, surface types, and time of concentration have large impacts on the results. For example, the site at RIS received runoff from a large grassed area and the results are therefore not necessarily applicable for cells in dense urban settings with catchments recognized by a high fraction of impermeable area and shorter time of concentration. Further testing and evaluation of cell size equations on existing cells in various catchments and climatic zones are therefore needed.

Certainly, more research is needed regarding the K_{sat} values of various bioretention media compositions and vegetation. Particularly, there is a need to report infiltration rates in existing bioretention cells together with the above-mentioned factors. Additionally, it is necessary to evaluate the effects of salt-laden stormwater on the K_{sat} values in the cells and, furthermore, how design or media composition can be altered to counteract any negative effects caused by road salt exposure.

CONCLUSIONS

Hydrological data from three bioretention cells located in cold climates were analyzed to evaluate the seasonal effects of temperature on the K_{sat} value and the hydrological performance, and test simple size equations for cold climate bioretention cells.

Certainly, the capacity of a bioretention cell to infiltrate water is a complex process influenced by the initial water content of the bioretention media, the capillary suction, and the pressure head from the ponded water. However, results from this study indicate that the hydrological performance of a cell can be predicted with relatively high precision by using a simplified equation which includes only a few parameters: the cell surface area (A_{bio}), the mean K_{sat} value of the bioretention media, and the maximum level of water on the surface (h_{max}). Owing to the limited number of cells evaluated in this study, more work is needed in order to validate if the equation can be used to size and design well-functioning bioretention cells. In particular, there is a need to investigate to what extent the size equation is capable of predicting the hydrological performance of cells other than those tested in this study. Furthermore, more knowledge is needed about how to achieve the targeted K_{sat} value of the bioretention media when designing new cells. Finally, there is a need to address to what extent exposure of road salts can cause reductions in the K_{sat} value in bioretention cells operated in cold climate regions.

This study shows that bioretention cells operated in regions with cold climates can, if the bioretention media have a low hydraulic capacity, be subject to significant seasonal variability in hydrological performance. In order to account for the seasonal variability value, bioretention media with a sufficiently high K_{sat} value (i.e., >10 cm/h)

should be targeted when designing bioretention cells for optimal hydrologic performance in cold climate regions.

ACKNOWLEDGEMENTS

REFERENCES

Archer, N. A. L., Quinton, J. N. & Hess, T. M. 2002 Below-ground relationships of soil texture, roots and hydraulic conductivity in two-phase mosaic vegetation in South-east Spain. *J. Arid Environ.* **52** (4), 535–553.

Asare, S. N., Rudra, R. P., Dickinson, W. T. & Wall, G. J. 1999 Effect of freeze-thaw cycle on the parameters of the Green and Ampt infiltration equation. *J. Agr. Eng. Res.* **73** (3), 265–274.

Asleson, B. C., Nestingen, R. S., Gulliver, J. S., Hozalski, R. M. & Nieber, J. L. 2009 Performance assessment of rain gardens. *J. Am. Water Resour. Assoc.* **45** (4), 1019–1031.

Austin (2015) Section 1 – Water quality management. In: *Austin, Texas – Environmental Criteria Manual*. City of Austin, Texas, USA. Available at: https://www.municode.com/library/tx/austin/codes/environmental_criteria_manual?nodeId=15306 Accessed 8 October 2015.

Blecken, G.-T., Marsalek, J. & Viklander, M. 2011 Laboratory study of stormwater biofiltration in low temperatures: total and dissolved metal removals and fates. *Water Air Soil Pollut.* **219** (1–4), 303–317.

Blecken, G.-T., Zinger, Y., Muthanna, T., Deletic, A., Fletcher, T. & Viklander, M. 2007 The influence of temperature on nutrient treatment efficiency in stormwater biofilter systems. *Water Sci. Technol.* **56** (10), 83–91.

Braga, A., Horst, M. & Traver, R. G. 2007 Temperature effects on the infiltration rate through an infiltration basin BMP. *ASCE J. Irrig. Drain. Eng.* **133** (6), 593–601.

Braskerud, B. C., Paus, K. H. & Ekle, A. 2013 Constructing raingardens. A pictorial cavalcade over 4 constructed raingardens in Norway. NVE report 3/2013, Oslo, Norway (in Norwegian with extended English summary). Available from: http://webby.nve.no/publikasjoner/rapport/2013/rapport2013_03.pdf.

Caraco, D. & Claytor, R. 1997 *Stormwater BMP Design Supplement for Cold Climates*. Center for Watershed Protection, Ellicott City, Maryland, USA.

Claytor, R. A. & Schueler, T. R. 1996 *Design of Stormwater Filtering Systems*. Chesepeake Research Consortium, The Center for Watershed Protection, Ellicott City, Maryland, USA.

Crowe, C. T., Elger, D. F. & Roberson, J. A. 2005 *Engineering Fluid Mechanics*. John Wiley & Sons, Hoboken, New Jersey, USA.

Davis, A. P. 2008 Field performance of bioretention: hydrology impacts. *J. Hydrol. Eng.* **13** (2), 90–95.

Davis, A. P., Hunt, W. F., Traver, R. G. & Clar, M. 2009 Bioretention technology overview of current practice and future needs. *J. Environ. Eng.* **135** (3), 109–117.

Davis, A. P., Shokouhian, M., Sharma, H., Minami, C. & Winogradoff, D. 2003 Water quality improvement through bioretention: lead, copper, and zinc removal. *Water Environ. Res.* **78** (3), 284–293.

Emerson, C. H. 2008 *Evaluation of Infiltration Practices as a Means to Control Stormwater Runoff*. Villanova University, Philadelphia, Pennsylvania, USA.

Emerson, C. H. & Traver, R. G. 2008 Multiyear and seasonal variation of infiltration from storm-water best management practices. *ASCE J. Irrig. Drain. Eng.* **134** (5), 598–605.

Gregory, J. H., Dukes, M. D., Jones, P. H. & Miller, G. L. 2006 Effect of urban soil compaction on infiltration rate. *J. Soil Water Conserv.* **61** (3), 117–124.

Hatt, B. E., Fletcher, T. D. & Deletic, A. 2009 Hydrologic and pollutant removal performance of stormwater biofiltration systems at the field scale. *J. Hydrol.* **365** (3–4), 310–321.

Hillel, D. 1998 *Environmental Soil Physics*. Academic Press, San Diego, California, USA.

Hudson, B. D. 1994 Soil organic-matter and available water capacity. *J. Soil Water Conserv.* **49** (2), 189–194.

Hunt, W. F. & White, N. 2001 *Urban waterways: designing rain gardens (bioretention areas)*. North Carolina Cooperative Extension Service, Report no. AG-588-3, Raleigh, North Carolina, USA.

Hunt, W. F., Jarrett, A. R., Smith, J. T. & Sharkey, L. J. 2006 Evaluating bioretention hydrology and nutrient removal at three field sites in North Carolina. *ASCE J. Irrig. Drain. Eng.* **132** (6), 600–608.

Hunt, W. F., Smith, J. T., Jadlocki, S. J., Hathaway, J. M. & Eubanks, P. R. 2008 Pollutant removal and peak flow mitigation by a bioretention cell in urban Charlotte, N.C. *J. Environ. Eng.* **134** (5), 403–408.

Kakuturu, S. P. & Clark, S. E. 2015 Clogging mechanism of stormwater filter media by NaCl as a deicing salt. *Environ. Eng. Sci.* **32** (2), 141–152.

Khan, U. T., Valeo, C., Chu, A. & van Duin, B. 2012 Bioretention cell efficacy in cold climates: part 1 – hydrologic performance. *Can. J. Civil Eng.* **39** (11), 1210–1221.

Krogstad, T. 1992 *Methods for soil analysis* (in Norwegian), NLH report no. 6, Institutt for jordfag, Ås-NHL.

Lamande, M., Hallaire, V., Curmi, P., Peres, G. & Cluzeau, D. 2003 Changes of pore morphology, infiltration and earthworm community in a loamy soil under different agricultural managements. *Catena* **54** (3), 637–649.

Langergraber, G., Haberl, R., Laber, J. & Pressl, A. 2003 Evaluation of substrate clogging processes in vertical flow constructed wetlands. *Water Sci. Technol.* **48** (5), 25–34.

Le Coustumer, S., Fletcher, T. D., Deletic, A., Barraud, S. & Lewis, J. F. 2009 Hydraulic performance of biofilter systems for stormwater management: influences of design and operation. *J. Hydrol.* **376** (1–2), 16–23.

LeFevre, N. J., Davidson, J. D. & Oberts, G. L. 2009 Bioretention of simulated snowmelt: Cold climate performance and design criteria. In: *14th Conference on Cold Regions Engineering*, Duluth, Minnesota, USA, pp. 145–154.

LeFevre, G. H., Novak, P. J. & Hozalski, R. H. 2012 Fate of naphthalene in laboratory-scale bioretention cells: implications for sustainable stormwater management. *Environ. Sci. Technol.* **46** (2), 995–1002.

LeFevre, G. H., Paus, K. H., Natarajan, P., Gulliver, J. S., Novak, P. J. & Hozalski, R. M. 2014 A review of dissolved pollutants in urban stormwater and their removal and fate in bioretention cells. *J. Environ. Eng.* **141** (1), doi:10.1061/(ASCE)EE.1943-7870.0000876.

Li, H. & Davis, A. P. 2008 Urban particle capture in bioretention media. I: Laboratory and field studies. *J. Environ. Eng.* **134** (6), 409–418.

Minitab 2010 *Minitab Statistical Software Version 16.1.0.* Minitab Inc., State College, Pennsylvania, USA.

Muthanna, T. M., Viklander, M., Gjesdahl, N. & Thorolfsson, S. T. 2007 Heavy metal removal in cold climate bioretention. *Water Air Soil Pollut.* **183** (1), 391–402.

Muthanna, T. M., Viklander, M. & Thorolfsson, S. T. 2008 Seasonal climatic effects on the hydrology of a rain garden. *Hydrol. Process.* **22** (11), 1640–1649.

Nestingen, R. S. 2007 The comparison of infiltration devices and modification of the Philip-Dunne permeameter for the assessment of rain gardens. MSc Thesis, Department of Civil Engineering, University of Minnesota, Minneapolis, USA.

NYSDEC 2010 *New York State Stormwater Management Design Manual.* New York State Department of Environmental Conservation, Albany, New York, USA.

Paus, K. H. & Braskerud, B. C. 2014 Suggestions for designing and building bioretention cells for Nordic conditions. *VATTEN J. Water Manage. Res.* **70**, 139–150.

Paus, K. H., Morgan, J., Gulliver, J. S. & Hozalski, R. M. 2014a Effects of bioretention media compost volume fraction on toxic metals removal, hydraulic conductivity, and phosphorous release. *J. Environ. Eng.* **140** (10), doi: 10.1061/(ASCE)EE.1943-7870.0000846.

Paus, K. H., Morgan, J., Gulliver, J. S., Leikness, T. & Hozalski, R. M. 2014b Assessment of the hydraulic and toxic metal removal capacities of bioretention cells after 2 to 8 years of service. *Water Air Soil Pollut.* **225** (1), doi:10.1007/s11270-013-1803-y.

Paus, K. H., Morgan, J., Gulliver, J. S., Leikness, T. & Hozalski, R. M. 2014c Effects of temperature and NaCl on toxic metal retention in bioretention media. *J. Environ. Eng.* **140** (10), doi: 10.1061/(ASCE)EE.1943-7870.0000847.

PGC 2007 *Bioretention Manual.* Environmental Service Division, Department of Environmental Resources, Prince George's County, Maryland, USA.

Saxton, K. E. & Rawls, W. J. 2006 Soil water characteristic estimates by texture and organic matter for hydrologic solutions. *Soil Sci. Soc. Am. J.* **70** (5), 1569–1578.

Søberg, L., Blecken, G.-T. & Viklander, M. 2014 The influence of temperature and salt on metal and sediment removal in stormwater biofilters. *Water Sci. Technol.* **69** (11), 2295–2304.

Szota, C., Farrell, C., Livesley, S. J. & Fletcher, T. D. 2015 Salt tolerant plants increase nitrogen removal from biofiltration systems affected by saline stormwater. *Water Res.* **83**, 195–204.

Thompson, A. M., Paul, A. C. & Balster, N. J. 2008 Physical and hydraulic properties of engineered soil media for bioretention basins. *Trans. ASABE* **51** (2), 499–514.